The Journal of Chemical Physics ARTICLE pubs.aip.org/aip/jcp

Ordering properties of anisotropic hard bodies in one-dimensional channels

Cite as: J. Chem. Phys. 159, 154507 (2023); doi: 10.1063/5.0169605
Submitted: 27 July 2023 • Accepted: 26 September 2023 •
Published Online: 20 October 2023

Ana M. Montero,[1,a] Andrés Santos,[1,2,b] Péter Gurin,[3,c] and Szabolcs Varga[3,d]

AFFILIATIONS

[1] Departamento de Física, Universidad de Extremadura, E-06006 Badajoz, Spain
[2] Instituto de Computación Científica Avanzada (ICCAEx), Universidad de Extremadura, E-06006 Badajoz, Spain
[3] Physics Department, Centre for Natural Sciences, University of Pannonia, P.O. Box 158, Veszprém H-8201, Hungary

[a] **Author to whom correspondence should be addressed:** anamontero@unex.es
[b] **Electronic mail:** andres@unex.es
[c] **Electronic mail:** gurin.peter@mk.uni-pannon.hu
[d] **Electronic mail:** varga.szabolcs@mk.uni-pannon.hu

ABSTRACT

The phase behavior and structural properties of hard anisotropic particles (prisms and dumbbells) are examined in one-dimensional channels using the Parsons–Lee (PL) theory, and the transfer-matrix and neighbor-distribution methods. The particles are allowed to move freely along the channel, while their orientations are constrained such that one particle can occupy only two or three different lengths along the channel. In this confinement setting, hard prisms behave as an additive mixture, while hard dumbbells behave as a non-additive one. We prove that all methods provide exact results for the phase properties of hard prisms, while only the neighbor-distribution and transfer-matrix methods are exact for hard dumbbells. This shows that non-additive effects are incorrectly included into the PL theory, which is a successful theory of the isotropic-nematic phase transition of rod-like particles in higher dimensions. In the one-dimensional channel, the orientational ordering develops continuously with increasing density, i.e., the system is isotropic only at zero density, while it becomes perfectly ordered at the close-packing density. We show that there is no orientational correlation in the hard prism system, while the hard dumbbells are orientationally correlated with diverging correlation length at close packing. On the other hand, positional correlations are present for all the systems, the associated correlation length diverging at close packing.

I. INTRODUCTION

It is generally accepted that hard-body interactions play a key role in the structural properties and phase behavior of molecular liquids, colloids and soft matter.[1] In addition to this, the shape of the particles is also important, as the anisotropic shape is responsible for the stabilization of complex meso- and crystalline structures.[2]

Moreover, geometric confinements (e.g., pores and channels) and interfacial confinements (e.g., particles at solid–liquid, liquid–liquid, and gas–liquid interfaces) complicate further the ordering and phase properties of the particles.[3,4]

Of particular interest are quasi-one-dimensional (q1D) systems, in which particles form a necklace-like structure in either side-by-side or end-to-end configurations, in such a way that all particles are trapped between their first neighbors.[5,6] In such an environment, and if the interaction range is short enough, the phase behavior of the system is very different from that of three-dimensional bulk, since each particle interacts only with its first neighbors and the confining wall.[7,8] For example, water molecules cannot form H-bonding networks in q1D ultaconfinement, which changes several properties of water dramatically, such as the conductivity, the diffusivity, and the fluid structure.[9] Similar changes occur in colloidal and soft matter systems in q1D confinements, where the shape of the particles can be rod-like or plate-like.[10]

Therefore, it is not surprising that the changes arising in physical and chemical properties make q1D systems very attractive for both practical and theoretical studies. A practical importance of q1D systems is that the necklace-like nanostructures from rod-like and plate-like building-blocks of semiconducting nanoparticles have outstanding quantum properties, which offer new electric and

optical applications in nanotechnology.[11] They can also be used in biological and chemical sensing due to their anisotropic properties, because they can be embedded into solid matrices.[12] The theoretical importance of these systems is that some fundamental issues can be addressed by studying q1D systems. These issues are, for instance, the existence or nonexistence of first-order phase transitions,[13,14] glass formation,[15,16] jamming,[17,18] or the possibility of long-range order in low dimensional systems.[19]

The minimal model of q1D necklace-like structures is made of hard-body building blocks, where the particles (building blocks) can be either spherical or anisotropic, can rotate to some extent, but are restricted to a straight line.[20] The system of strictly confined hard spheres corresponds to a one-dimensional (1D) system of hard rods, where the length of the rod is equal to the diameter of the sphere. This system belongs to the class of exactly solvable models, i.e., the equation of state, the pair distribution function, the percolation length, and several other thermodynamic and structural properties of 1D hard rods are analytical.[21–24] The general feature of 1D hard rods is that the pressure and the pair correlation length diverge at the close-packing density, but no phase transition occurs in the entire range of density.[25] Interestingly, this system can also be realized experimentally to study some dynamical and structural properties, such as the diffusion coefficient, the structure factor, and the pair correlation function.[26–30]

To induce a true phase transition, either a long-range attractive interaction should be added to the excluded volume interactions, like in the case of van der Waals theory,[31,32] or anisotropic particles should be placed on a 1D lattice with some degree of orientational freedom.[33–36] In general, q1D systems of hard anisotropic particles with rotational freedom do not belong to the class of analytically solvable models, but the thermodynamic properties and the pair correlation functions can be determined exactly by the numerical solution of an eigenvalue equation coming from the transfer-matrix method.[37–40] In this regard, the exceptions are q1D additive hard-body systems, where the equation of state and the direct correlation function can be obtained analytically.[41,42] Adding some out-of-line positional freedom to the particles can lead to structural transitions, jamming, and glassy behavior. In the case of hard spheres, a weak fluid-zigzag structural transition takes place with increasing density[43–51] and, additionally, the presence of special jammed states shows the existence of glass-like structures.[52–55] Moreover, the correlation lengths diverge at the close-packing density as infinitely long zigzag order evolves.[56] If the shape of the hard particle is anisotropic, the competition between fluid-like and solid-like structures gives rise to anomalous structural transition, which looks like a first-order phase transition.[57] In addition to this, the phase behavior of both spherical and non-spherical hard-body fluids becomes very complex by allowing the particles to pass each other, since tilted, chiral, and achiral structures become the close-packing structure by changing the size of the pore.[58–61]

To test the reliability of approximate theoretical methods, such as the classical density functional theory (DFT) and the integral-equation approximations, which are devised for two- and three-dimensional systems, 1D and q1D systems with short-range interactions can be considered as an ideal playground, since the output of these theories can be compared with the exact results coming from transfer-matrix (TM) and neighbor-distribution (ND) methods. The former approximate theories have the advantage that they can be easily generalized to higher dimensions, while the extension of exact methods is still challenging, even in one dimension, if the pair interaction is not restricted to the first neighbor.[62] The TM and ND methods proved to be very successful for 1D and q1D systems with continuous positional and orientational freedom, such as the fluid of hard needles[17,38] and that of hard disks.[43,51] Note that the freely rotating hard needles can be considered as a simple model of liquid crystals in one dimension[40] and even the liquid crystal elastomers can be studied with the inclusion of harmonic elastic forces between the neighboring needles.[63] Regarding the development of DFT, exact functionals have been derived only for hard rods[64] and hard-rod mixtures,[65] while even the fundamental-measure density functional is approximate for non-additive mixtures.[66] The problems, failures, and challenges in obtaining accurate DFT of non-additive and q1D fluids are reviewed in Refs. 67 and 68.

Another possibility to study q1D systems is to use the Parsons–Lee (PL) theory,[69,70] which is also approximate, but it proved to be quite accurate for describing the orientational ordering properties and the isotropic-nematic transition of hard nonspherical particles in two and three dimensions.[71–73] Interestingly, its success is poorly understood for the equation of state and the transition densities of isotropic-nematic phase transition. Moreover, to our knowledge, its applicability has not been studied in one dimension yet. Therefore, one can get some insight into the success of the PL theory by studying some 1D hard-body fluids, where the shape of the particle can be both convex and concave.

In this study, we examine the phase behavior and structural properties of q1D hard-body fluids, where the shape of the particle is rod-like. The particles are placed into a very narrow channel with either rectangular or circular cross section, where they form a single-file fluid with only first-neighbor interactions. The effect of out-of-line positional freedom is completely neglected, i.e., the particles are allowed to move freely only in one spatial dimension, while the out-of-line orientational freedom is restricted to two and three states in rectangular and circular channels, respectively. We show that hard prisms behave as an additive mixture, where all components have the same chemical potential. Contrary to this, the hard dumbbells can be represented as a non-additive mixture with the same constraint for the chemical potentials. Both systems exhibit orientational ordering with increasing density, where the phase is isotropic only at vanishing density. The fluid of hard prisms becomes identical with that of hard rods at close packing, where the shortest length of the prism along the channel corresponds to the diameter of the rod. This system can be characterized by diverging positional correlation at close packing, while it lacks orientational correlation. The phase behavior of hard dumbbells is very different because it forms crossed structures at high densities, where the angle between the neighboring particles is 90°. Moreover, the dumbbells are more ordered since both the positional and orientational correlation lengths diverge at close packing. We show that the PL theory, which is devised for isotropic and nematic phases of two- and three-dimensional hard-body fluids, is exact for additive q1D fluids, regardless of the number of orientations, while it is only approximate for non-additive ones. To take into account exactly the effect of non-additive interactions, TM or ND methods should be used. In addition, these two exact methods complement each other because the ND method provides information about the changes occurring in the positional order, while the TM method is

more suitable to study the orientational ordering properties of the system.

The organization of this paper is as follows. The prism and dumbbell models are presented in Sec. II. Then, Sec. III is devoted to the PL theory and the exact TM and ND methods. The results for the bulk properties, the pair distribution function, and the correlation lengths (both orientational and positional) are presented and discussed in Sec. IV. Finally, Sec. V offers the main conclusions of the paper.

II. MODELS

We use simple hard-body models for our q1D study, where the possible orientations of the particles are restricted to two or three orientations only, as sketched in Fig. 1. We assume that the centers of the particles are restricted to the z axis, but the particles can move freely along this axis. The particles are not allowed to overlap as they are hard objects. We can see in Fig. 1 that the occupied length of the particle can be σ_1, σ_2, and σ_3 along the z axis as the particle can orient its largest length along the x, y, and z axes, respectively. For the sake of simplicity, we assume that $\sigma_1 \le \sigma_2 \le \sigma_3$ for hard prisms and $\sigma_1 = \sigma, \sigma_2 = \sigma$, and $\sigma_3 = 2\sigma$ for hard dumbbells. We measure all lengths and make all quantities dimensionless with σ_1, which is then the unit of length. The hard prisms are additive, because the contact distance between two prisms is given by $\sigma_{ij} = (\sigma_j + \sigma_j)/2$ for any pair of orientations $(i, j = 1, 2, 3)$. This is not true for hard dumbbells because $\sigma_{ij} \neq (\sigma_j + \sigma_j)/2$ for $i \neq j$; more specifically, $\sigma_{12}/\sigma = 1/\sqrt{2} \simeq 0.707$ and $\sigma_{13}/\sigma = \sigma_{23}/\sigma = (1 + \sqrt{3})/2 \simeq 1.366$. With these two models we can examine the effects of additive and non-additive hard-body interactions.

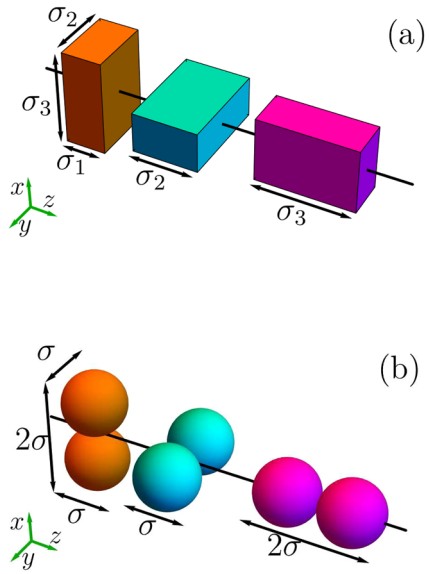

FIG. 1. Schematics of (a) hard prisms and (b) hard dumbbells in q1D channels. The particles are allowed to orient along x, y, and z axis with the corresponding lengths (σ_1, σ_2, and σ_3) along the z axis. In the case of dumbbells, $\sigma_1 = \sigma$, $\sigma_2 = \sigma$ and $\sigma_3 = 2\sigma$.

III. THEORY

In this section, we present three different theories for q1D hard-body fluids. In the three cases, the number n of internal states (or, in the mixture language, the number of components) is arbitrary. So are the lengths σ_i, the cross contact distances σ_{ij}, and the nature (additive or non-additive) of the interactions.

We start with the PL theory, which provides the equation of state and the fraction of particles (x_i) having length σ_i along the z axis. Then, we present the TM method for the exact calculation of the Gibbs free energy and other thermodynamic properties. In addition, we show that this method provides information about the orientational correlations along the z axis. Finally, we derive the exact equations for the orientation-dependent pair distribution function using the ND method.

A. Parsons–Lee (PL) theory

The easiest way to derive the PL theory from the three possible ways[74–76] is to start from the virial series of the excess free energy density F_{ex},

$$\frac{\beta F_{ex}}{L} = \sum_{i=2}^{\infty} \frac{B_i}{i-1} \rho^i, \tag{3.1}$$

where $\beta = 1/k_B T$ is the inverse temperature (k_B being the Boltzmann constant), L is the length of the channel, B_i is the ith virial coefficient, $\rho = N/L$ is the linear number density, and N is the number of particles in the channel. According to Lee's idea,[70] a mapping procedure can be made between the system of anisotropic particles and that of spherical particles through the virial coefficients. In the case of 1D confinement, the hard rods having length d can be used in the mapping procedure as follows,

$$B_i \approx \frac{B_2}{B_2^{\mathrm{R}}} B_i^{\mathrm{R}}, \tag{3.2}$$

where B_i^{R} denotes the ith virial coefficient of the hard rods. This equation assumes that the virial coefficients of the hard rods and those of anisotropic particles are proportional to each other. Substituting Eq. (3.2) into Eq. (3.1), we obtain, after simplification, that

$$F_{ex} = F_{ex}^{\mathrm{R}} \frac{B_2}{B_2^{\mathrm{R}}}, \tag{3.3}$$

where F_{ex}^{R} is the excess free energy of the hard rods. Due to Tonks,[21] this free energy term is analytically known as

$$\frac{\beta F_{ex}^{\mathrm{R}}}{L} = -\rho \ln(1 - \rho d). \tag{3.4}$$

Using an n-state representation of the possible orientations of the hard-body anisotropic particles, it can be shown that the second virial coefficient is given by

$$B_2 = \sum_{i,j=1}^{n} x_i x_j \sigma_{ij}. \tag{3.5}$$

In the case of hard rods, Eq. (3.5) simplifies to $B_2^{\mathrm{R}} = d$. Thus, Eqs. (3.3) and (3.4) yield

$$\frac{\beta F_{\mathrm{ex}}}{L} = -\rho \ln(1-\rho d)\, \frac{1}{d}\sum_{i,j=1}^{n} x_i x_j \sigma_{ij}. \tag{3.6}$$

To complete the determination of the excess free energy, a relationship between the hard-rod length d and the lengths $\{\sigma_{ij}\}$ of the anisotropic particles is needed. A natural choice is $d = \langle\sigma\rangle = \sum_{i=1}^{n} x_i\sigma_i$, which ensures that the occupied length of the rods and that of the anisotropic particles are the same along the z axis in the case of additive cross interactions. Here we note that the generalization of Eq. (3.6) is straightforward in higher dimensions as the hard disk and sphere can be used as a reference mapping particle in two and three dimensions, respectively. The total free energy, which is the sum of ideal and excess terms ($F = F_{\mathrm{id}} + F_{\mathrm{ex}}$), can be written as

$$\frac{\beta F}{L} = \sum_{i=1}^{n} \rho_i(\ln\rho_i - 1) - \frac{\ln(1-\eta)}{\eta}\sum_{i,j=1}^{n}\rho_i\rho_j\sigma_{ij}, \tag{3.7}$$

where $\rho_i = \rho x_i$ is the density of component i and $\eta = \sum_{i=1}^{n}\rho_i\sigma_i = \rho d = \rho\langle\sigma\rangle$ is the linear packing fraction. Here, without loss of generality, we have taken the thermal de Broglie wavelength equal to unity. The chemical potential of component i and the pressure can be obtained from Eq. (3.7) using standard thermodynamic relations as follows,

$$\beta\mu_i = \frac{\partial(\beta F/L)}{\partial\rho_i}, \quad (i = 1,\ldots n), \tag{3.8a}$$

$$\beta P = -\frac{\beta F}{L} + \sum_{i=1}^{n}\beta\mu_i\rho_i. \tag{3.8b}$$

In the case of additive excluded length, one has $\sum_{i,j=1}^{n}\rho_i\rho_j\sigma_{ij} = \rho\eta$, so that the total free energy simplifies to

$$\frac{\beta F}{L} = \sum_{i=1}^{n}\rho_i(\ln\rho_i - 1) - \rho\ln(1-\eta). \tag{3.9}$$

From this equation one gets the chemical potentials and the pressure using Eq. (3.8), i.e.,

$$\beta\mu_i = \ln\rho_i - \ln(1-\eta) + \frac{\rho\sigma_i}{1-\eta}, \tag{3.10a}$$

$$\beta P = \frac{\rho}{1-\eta}. \tag{3.10b}$$

The fraction of particles can be obtained from the condition that the chemical potential of all components are fixed to a given value (μ),[77] i.e., $\mu = \mu_1 = \cdots = \mu_n$. Therefore, in the case of additive interactions, we have

$$x_i = \frac{e^{-\rho\sigma_i/(1-\eta)}}{\sum_{j=1}^{n} e^{-\rho\sigma_j/(1-\eta)}}. \tag{3.11}$$

Note that this actually represents a set of transcendental equations for $\{x_i\}$, since η depends on $\{x_i\}$. Thus, it is not possible to provide a closed formula for x_i as a function of ρ. However, the density dependence of Eq. (3.11) can be replaced with the pressure one using Eq. (3.10b). The result is

$$x_i = \frac{e^{-\beta P\sigma_i}}{\sum_{j=1}^{n} e^{-\beta P\sigma_j}}. \tag{3.12}$$

Using Eq. (3.10), one can express the chemical potential, density, and packing fraction as functions of pressure:

$$\beta\mu = \ln(\beta P) - \ln\sum_{i=1}^{n} e^{-\beta P\sigma_i}, \tag{3.13a}$$

$$\rho^{-1} = \frac{\sum_{i=1}^{n}\sigma_i e^{-\beta P\sigma_i}}{\sum_{i=1}^{n} e^{-\beta P\sigma_i}} + \frac{1}{\beta P}, \tag{3.13b}$$

$$\eta = \frac{\beta P\sum_{i=1}^{n}\sigma_i e^{-\beta P\sigma_i}}{\sum_{i=1}^{n}(1+\beta P\sigma_i)e^{-\beta P\sigma_i}}. \tag{3.13c}$$

These results show that the pressure is the natural input of 1D additive systems, which is consistent with the TM and ND methods.

It is worth mentioning that Eq. (3.13) can be reproduced from the virial theorem using the decoupling approximation of the positional and orientational degrees of freedom.[74] In this approximation, the following three steps are used: (1) the pair potential of anisotropic hard bodies (u_{ij}) is scaled into that of hard rods, i.e., $u_{ij}(z) = u(zd/\sigma_{ij})$, where z is the distance between two particles, (2) the pair distribution function can be determined from $g_{ij}(z,\rho) \approx g^{\mathrm{R}}(zd/\sigma_{ij},\rho)$, where g^{R} is the pair distribution function of hard rods, and (3) the occupied distance of the particles equals to that of hard rods.

We finally note that the PL theory for the non-additive case, i.e., $\sigma_{ij} \neq (\sigma_i + \sigma_j)/2$, does not produce analytical results for the fractions x_i and the thermodynamic quantities.

B. Transfer-matrix (TM) method

The simplest way to determine the partition function and the derived thermodynamic quantities of q1D systems is to work in the isothermal-isobaric ensemble, where the partition function can be factorized as a product of matrices given by

$$K_{ij} = \frac{e^{-\beta P\sigma_{ij}}}{\beta P}, \tag{3.14}$$

where, as said before, σ_{ij} is the contact distance between two neighboring particles having i and j orientations, respectively. According to the TM method, the important quantities are the eigenvalues and the corresponding eigenvectors of the matrix K_{ij}. In the n-state system, the eigenvalue equation is given by

$$\sum_{j=1}^{n} K_{ij}\psi_j^{(k)} = \lambda_k\psi_i^{(k)}, \tag{3.15}$$

where λ_k is the kth eigenvalue, while $\psi_i^{(k)}$ is the ith component of the corresponding eigenvector. One gets the eigenvalues from the condition that the determinant of the matrix $K_{ij} - \lambda\delta_{ij}$ must be zero, while

the corresponding eigenvectors are obtained from the eigenvalue equation, Eq. (3.15). If the eigenvectors are normalized, then

$$\lambda_k = \sum_{i,j=1}^{n} K_{ij}\psi_i^{(k)}\psi_j^{(k)}. \tag{3.16}$$

From here, it is easy to prove[50] that

$$\frac{\partial(\beta P\lambda)}{\partial\beta P} = -\beta P\sum_{i,j=1}^{n} K_{ij}\sigma_{ij}\psi_i\psi_j, \tag{3.17}$$

where $\lambda = \max(\lambda_1,\ldots,\lambda_n)$ and ψ_i is the corresponding eigenvector.

The Gibbs free energy can be obtained from $\beta G/N = -\ln\lambda$. The equation of state, which connects the pressure and the density, is given by

$$\frac{1}{\rho} = \frac{\partial\beta G/N}{\partial\beta P} = -\frac{1}{\lambda}\frac{\partial\lambda}{\partial\beta P} = \frac{1}{\beta P} + \frac{1}{\lambda}\sum_{i,j=1}^{n} K_{ij}\sigma_{ij}\psi_i\psi_j, \tag{3.18}$$

where Eq. (3.17) has been used. Further information about the ordering can be gained from the (normalized) eigenfunction ψ_i, since the fraction of particles having a length σ_i along the z axis is $x_i = \psi_i^2$. Moreover, the orientational correlation between two pairs can be characterized with the help of the orientational correlation length (ξ_o),[40] which is obtained from the two largest eigenvalues as

$$\xi_o^{-1} = \ln\frac{\lambda}{|\lambda^*|}, \tag{3.19}$$

where λ^* is the second largest eigenvalue (in absolute value) of K_{ij}.

In the additive case, i.e., $\sigma_{ij} = (\sigma_i + \sigma_j)/2$, the eigenvalues and the eigenvectors can be obtained easily, because the matrix elements can be factorized as follows,

$$K_{ij} = \sqrt{K_i K_j}, \tag{3.20}$$

where $K_i = K_{ii} = e^{-\beta P\sigma_i}/\beta P$. Inserting Eq. (3.20) into Eq. (3.15) one gets that

$$\lambda_k\psi_i^{(k)} = \sqrt{K_i}\sum_{j=1}^{n}\sqrt{K_j}\psi_j^{(k)}. \tag{3.21}$$

Actually, Eq. (3.20) expresses that the matrix K_{ij} is the Kronecker product of a vector $\sqrt{K_i}$ by itself. As a consequence, apart from a constant multiplier, K_{ij} is the matrix of a rank 1 projector, and therefore, all its eigenvalues are zero except one, which is the largest, $\lambda = \sum_{i=1}^{n} K_i$; moreover, the corresponding eigenvector is proportional to the vector $\sqrt{K_i}$. From the normalization condition we have

$$x_i = \frac{K_i}{\sum_{j=1}^{n} K_j} = \frac{e^{-\beta P\sigma_i}}{\sum_{j=1}^{n} e^{-\beta P\sigma_j}}, \tag{3.22}$$

which is identical to Eq. (3.12) of the PL theory. It is easy to show that the TM method provides the same results for the equation of state, the packing fraction, and the chemical potential as that of the PL theory for arbitrary n and $\{\sigma_i\}$ provided the interactions are additive.

As the TM method is exact, it turns out that the PL theory is also an exact theory for q1D n-state hard-body systems in the additive case. At this point it is worth noting that the PL theory provides only the thermodynamic properties, while the TM method can be used to determine the structural properties, too. For example, Eq. (3.19) shows that there is no orientational correlation between the particles, i.e., the orientational correlation length is zero for additive systems because $\lambda^* = 0$.

As far as non-additive systems are concerned, the matrix element K_{ij} cannot be factorized as a product of two one-body terms, as in Eq. (3.20). Therefore, the resulting equations are more complicated for the ordering and thermodynamic properties, since the determinant of the matrix $K_{ij} - \lambda\delta_{ij}$ becomes an nth-order polynomial with nonzero eigenvalues $\lambda_1,\ldots,\lambda_n$. Using these exact results, we will show that the PL theory is not exact for non-additive systems.

C. Neighbor-distribution (ND) method

The complete determination of the physical properties of the system requires the knowledge of the pair distribution function $g_{ij}(z)$, which is proportional to the probability of finding a particle at position z and with orientation j, given that a particle with orientation i is located at the origin ($z = 0$).

To calculate $g_{ij}(z)$ in q1D systems, one needs to use the isothermal-isobaric ensemble and start from the determination of the nearest-neighbor probability distribution function, from which the ℓth-neighbor distribution function can be obtained by iterated convolutions. For this reason, here we will refer to this methodology as the ND method. In addition to $g_{ij}(z)$, the equation of state and other thermodynamic quantities can be calculated with it, yielding exactly the same results as those from the TM method. A drawback of the ND method is, however, that it does not provide information about the orientational correlations.

In this section, we summarize the main results derived from the ND method and refer the reader to Chap. 5 of Ref. 78 and, especially, Sec. III of Ref. 51 for further details. The exact pair distribution function is

$$g_{ij}(z) = \frac{1}{\rho\sqrt{x_i x_j}}\sum_{\ell=1}^{\lfloor z/\sigma_{\min}\rfloor}\frac{Q_{ij}^{(\ell)}(z)}{\lambda^{\ell}}, \tag{3.23}$$

where

$$Q_{ij}^{(1)}(z) = R^{(1)}(z;\sigma_{ij}), \tag{3.24a}$$

$$Q_{ij}^{(\ell)}(z) = \sum_{k_1=1}^{n}\sum_{k_2=1}^{n}\cdots\sum_{k_{\ell-1}=1}^{n} R^{(\ell)}(z;\Sigma_{ik_1k_2\cdots k_{\ell-1}j}), \quad \ell \geq 2, \tag{3.24b}$$

with

$$\Sigma_{ik_1k_2\cdots k_{\ell-1}j} \equiv \sigma_{ik_1} + \sigma_{k_1k_2} + \cdots + \sigma_{k_{\ell-1}j}, \tag{3.25a}$$

$$R^{(\ell)}(z;\alpha) \equiv \frac{e^{-\beta Pz}}{(\ell-1)!}(z-\alpha)^{\ell-1}\Theta(z-\alpha). \tag{3.25b}$$

In the upper summation limit of Eq. (3.23), $\lfloor\cdots\rfloor$ denotes the floor function and $\sigma_{\min} = \min\{\sigma_{ij}\}$. Note that $g_{ij}(z)$ presents a jump at $z = \sigma_{ij}$, kinks at $z = \Sigma_{ik_1j}$ ($k_1 = 1,\ldots,n$), and, in general, singularities of order $\ell - 1$ at $z = \Sigma_{ik_1k_2\cdots k_{\ell-1}j}$.

The Laplace transform $\widetilde{G}_{ij}(s) = \int_0^\infty dz\, e^{-sz} g_{ij}(z)$ is given by[51]

$$\widetilde{G}_{ij}(s) = \frac{1}{\lambda\rho\sqrt{x_i x_j}}\left(\Omega(s+\beta P)\cdot\left[\mathsf{I} - \lambda^{-1}\Omega(s+\beta P)\right]^{-1}\right)_{ij}, \tag{3.26}$$

where $\Omega(s)$ is the $n \times n$ matrix with elements $\Omega_{ij}(s) = e^{-s\sigma_{ij}}/s$. Note that $K_{ij} = \Omega_{ij}(\beta P)$.

In the additive case, $\Omega_{ij}(s) = \sqrt{\Omega_i(s)\Omega_j(s)}$, where $\Omega_i(s) = \Omega_{ii}(s)$, and this simplifies Eq. (3.26). After simple algebra, one finds

$$\begin{aligned}\widetilde{G}_{ij}(s) &= \frac{1}{\rho\sqrt{x_i x_j}}\frac{\Omega_{ij}(s+\beta P)}{\lambda - \sum_{k=1}^n \Omega_k(s+\beta P)} \\ &= \frac{1}{\rho}\frac{\beta P}{s+\beta P}\frac{e^{-s\sigma_{ij}}}{1-\lambda^{-1}\sum_{k=1}^n \Omega_k(s+\beta P)},\end{aligned} \tag{3.27}$$

where in the second step we have taken into account that $x_i = e^{-\beta P\sigma_i}/\lambda\beta P$ in the additive case. The second equality in Eq. (3.27) implies that all the pair distribution functions $g_{ij}(z)$ for additive systems are the same if the origin is shifted to $z = \sigma_{ij}$,[66,79,80] i.e.,

$$g_{ij}(z) = f(z - \sigma_{ij}), \tag{3.28}$$

where the function $f(z)$ is common for all pairs. Also in the additive case, Eqs. (3.23) and (3.24) can still be used, but Eq. (3.25a) simplifies to

$$\Sigma_{ik_1k_2\cdots k_{\ell-1}j} = \sigma_{ij} + \sigma_{k_1} + \sigma_{k_2} + \cdots + \sigma_{k_{\ell-1}}. \tag{3.29}$$

The asymptotic decay of $g_{ij}(z) - 1$ is characterized by the nonzero poles of $\widetilde{G}_{ij}(s)$, i.e., the roots (different from $s = 0$) of the determinant of the matrix $\mathsf{I} - \lambda^{-1}\Omega(s+\beta P)$ for non-additive systems [see Eq. (3.26)] or of $1 - \lambda^{-1}\sum_{k=1}^n \Omega_k(s+\beta P)$ for additive systems [see Eq. (3.27)]. If we denote by $s_\pm = -\kappa \pm \imath\omega$ the pair of conjugate poles with the real part closest to the origin, its residue being $|\mathcal{A}_{ij}|e^{\pm\imath\delta_{ij}}$, then, for asymptotically large z,

$$g_{ij}(z) - 1 \approx 2|\mathcal{A}_{ij}|e^{-\kappa z}\cos(\omega z + \delta_{ij}). \tag{3.30}$$

Thus, $\xi_p = \kappa^{-1}$ represents the positional correlation length, whereas ω is the (angular) oscillation frequency. As density increases, the imaginary part (ω) can experience a discontinuous jump at a certain density, giving rise to a structural crossover from oscillations with a certain frequency to oscillations with a different one. The origin of this jump resides in the crossing of the real part of two competing poles with different imaginary parts.

IV. RESULTS

In this section, we present our results for the phase behavior and structural properties of hard prisms and dumbbells in q1D channels (see Fig. 1) using the PL theory, as well as the TM and ND methods. The particles are allowed to move freely along the channel, but their orientational freedom is restricted to either two ($n = 2$) or three ($n = 3$) orientations. The main difference between hard prisms and dumbbells is that the contact distance between two prisms is additive for any pairs of orientations, i.e., $\sigma_{ij} = (\sigma_j + \sigma_j)/2$, while hard dumbbells are non-additive as $\sigma_{ij} \neq (\sigma_j + \sigma_j)/2$ for $i \neq j$ orientations. We use the following dimensionless quantities: $z^* = z/\sigma_1$, $\rho^* = \rho\sigma_1$, and $P^* = \beta P\sigma_1$.

A. Bulk properties

1. Hard prisms

We start with the simple q1D fluid of hard prisms and compare the bulk properties of two-state and three-state models. It is easy to show that the prisms are parallel with their shortest length σ_1 along the z axis at close packing. Therefore, they must behave as a 1D fluid of hard rods at high densities, where $x_1 \to 1$ and $\eta \to \rho\sigma_1$ describe the phase properties of the system. In the low-density, ideal-gas limit, the particles form an isotropic phase in both models, with $x_i \to 1/n$ holding for the n-state model. This can be obtained from Eq. (3.11) or Eq. (3.22) by taking the limits $\rho \to 0$ or $\beta P \to 0$, respectively. We can see from these limiting results that the structure of hard prisms changes from isotropic to a perfect nematic fluid with increasing density. The results of Eqs. (3.11), (3.13b), and (3.13c) are shown together in Fig. 2.

Starting with the equation of state (P^* vs ρ^*), we can see in Fig. 2(a) that there are some differences in the resulting curves at intermediate densities, while the two-state and three-state prisms behave almost identically at very low and high densities. The low-density agreement is trivial because of the ideal-gas limit, but the high-density one is due to the orientational ordering of the prisms into the state with length σ_1 along the z axis. This can be seen clearly in Fig. 2(b), where x_1 goes to 1 with increasing density for both two- and three-state models. The effect of increasing density is that neighboring particles get closer to each other, which reduces the available room for the particles. To minimize the translational entropy loss, the particles reduce their length along the z axis with orientational ordering, which manifests in an orientational entropy

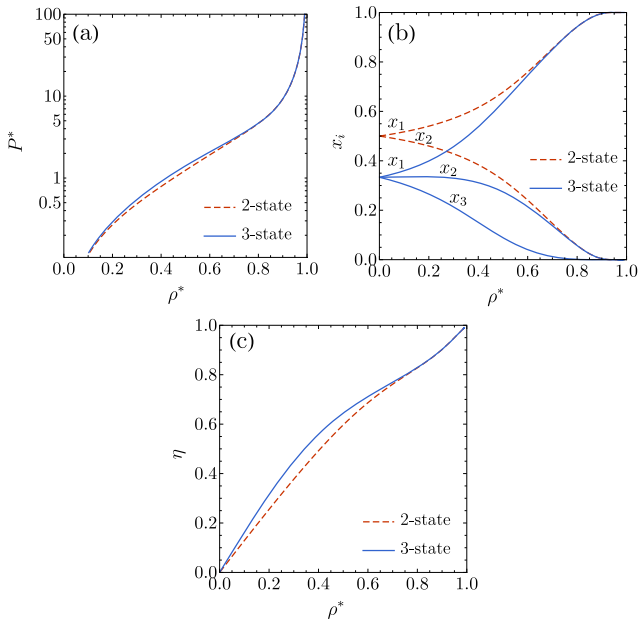

FIG. 2. Phase behavior of hard prisms in a q1D channel: (a) pressure, (b) mole fraction, and (c) packing fraction as functions of density. Particles can orient along the x and y axes only in the two-state model, while the x, y, and z axes are allowed in the three-state one. The lengths of the prism are chosen as follows: $\sigma_1 = 1$, $\sigma_2 = 1.6$, and $\sigma_3 = 2.4$. The pressure and density are dimensionless: $P^* = \beta P\sigma_1$ and $\rho^* = \rho\sigma_1$.

loss. Therefore, the competition between the translational and orientational entropies results in a continuous structural change from the isotropic to the perfectly ordered nematic fluid. It can be seen in Fig. 2(b) that the ordering is more pronounced for the three-state model than for the two-state one, since the translational entropy gain is higher as the number of particles having length σ_3 (which is the longest side of the prism) decreases. As the orientation with length σ_3 is missing in the two-state model, the changes are smoother in the two-state model than in the three-state one.

It is also obvious that the pressure and the packing fraction are higher in the three-state model than in the two-state one at a given density [see Figs. 2(a) and 2(c)] because the particles are always closer to each other in the three-state model since the orientational entropy makes $x_3 \neq 0$. The difference between the two models virtually disappears at $\rho^* = 0.8$, because x_3 is almost zero beyond this density. Moreover, both systems become almost a 1D fluid of hard rods with length σ_1 for $\rho^* > 0.9$, where x_2 and x_3 are practically zero. Note that the equation of state of 1D hard rods of length d, which is given by $\beta P = \rho/(1-\eta)$ with $\eta = \rho d$,[21] can describe n-state additive hard-body systems, such as the two- and three-state prisms, if $d = \langle\sigma\rangle$ is the average length of the particle along the z axis, as done in the PL theory [see Eq. (3.10b)]. In the light of this result, the curve η vs ρ^* measures the deviation from 1D hard rods, because the curve is a straight line for 1D hard rods since $\eta = \rho\sigma_1$ in that case. Figure 2(c) shows that the deviation from the 1D hard-rod system increases with the number of orientational states mainly at intermediate densities, while the n-state system converges toward the 1D hard-rod system at very high densities, where $\langle\sigma\rangle \approx \sigma_1$. These results show that the addition of more and more out-of-line orientational freedom to the system increases the deviation from the 1D fluid of hard rods.

2. Hard dumbbells

The phase behavior of q1D hard dumbbells is more complicated due to the presence of non-additive interactions. As the two hard spheres making a dumbbell are in contact (see Fig. 1), the length of the particle can be either σ (in states 1 and 2) or 2σ (in state 3) along the z axis. Keeping in mind the symmetry property of the contact distance ($\sigma_{ij} = \sigma_{ji}$), one can get all σ_{ij} using the following special values: $\sigma_{11} = \sigma_{22} = \sigma$, $\sigma_{33} = 2\sigma$, $\sigma_{12} = \sigma/\sqrt{2}$, and $\sigma_{13} = \sigma_{23} = (1+\sqrt{3})\sigma/2$. These contact distances and the pressure are the inputs of the exact TM and ND methods. Note that the input of the PL theory is the density and the effective length $d = \langle\sigma\rangle$. We examine the following two- and three-state systems: (a) a two-state model in which the state 1 with length σ and the state 3 with length 2σ are allowed, and (b) a three-state model where all states are included.

To understand the phase behavior of the q1D dumbbell fluid, it is worth considering the close-packing structure of the system. The possible shortest distance between two dumbbells is σ in the two-state model, i.e., one dumbbell occupies a distance σ and the close-packing density is given by $\rho_{cp} = 1/\sigma$. Therefore, the dumbbells are parallel at close packing and form a perfect nematic order with $x_1 = 1$. Consequently, the dumbbells behave as a 1D hard-rod fluid at high densities with $\beta P = \rho/(1-\eta)$ and $\eta = \rho\sigma$. This shows that the close-packing behavior of two-state dumbbells and that of prisms are the same. In the three-state model, however, the shortest distance between two dumbbells is given by $\sigma/\sqrt{2}$, i.e., the neighboring dumbbells must be perpendicular with respect to each other and both perpendicular to the z axis at close packing. This means that one dumbbell occupies a distance $\sigma/\sqrt{2}$ and the close-packing density is given by $\rho_{cp} = \sqrt{2}/\sigma$. This ordered structure is not planar nematic, because the order of particles with states 1 and 2 is not random along the z axis. Note that if two particles are parallel, the shortest distance between them is σ, which is higher than $\sigma/\sqrt{2}$. Therefore, the close-packed structure of the three-state dumbbell system is the sequence 1-2-1-2-$\cdots$ of the states along the z axis. We use the name "crossed" for this ordered structure because neighboring particles like to be perpendicular to each other. The consequence of the crossed ordering for the close-packing properties is that $x_1 = x_2 = 1/2$ and $\eta_{cp} = \sqrt{2}$.

From these results, we can see that, whereas $\eta = \rho\sum_{i=1}^{n} x_i\sigma_i$ is the real 1D packing fraction of additive systems, it is just a density-dependent quantity for non-additive ones. This fact has a serious consequence for the applicability of the PL theory because the PL excess free energy diverges at $\eta = 1$ [see Eq. (3.7)], which is below the maximal value ($\eta_{cp} = \sqrt{2}$) for the three-state dumbbell model. Therefore, the PL theory is not exact and is unable to predict the phase behavior of hard dumbbells if $\eta > 1$.

This shortcoming of the PL theory and the deviation from additive prism systems is illustrated in Fig. 3, where the exact and the PL results are shown together for the bulk properties of two- and three-state hard dumbbells.

In the two-state model, only the contact distance $\sigma_{13} \simeq 0.91 \times (\sigma_1 + \sigma_3)/2$ induces some negative non-additive effects in the results. Therefore, due to the very weak non-additive character of σ_{13}, the resulting equation of state and the ordering properties are almost identical with those of two-state hard prisms. Similarly to hard prisms, two-state hard dumbbells undergo a continuous structural change from the isotropic fluid to the perfectly ordered nematic one with increasing density. This can be seen clearly in Fig. 3(b), where the fraction of particles in state 1 (x_1) increases continuously from 0.5 to 1. In the two-state dumbbell model, η cannot be considered as a 1D packing fraction, but it becomes identical with the packing fraction of hard rods of length σ at high densities ($\rho^* > 0.8$). It can be seen in Fig. 3(c) that η is higher than the packing fraction of hard rods at intermediate densities since there are some dumbbells with length 2σ along the z axis. This positive deviation is due to the orientational entropy, which favors the orientational disorder. However, this entropy term weakens with increasing density due to the decreasing available room.

To analyze the deviation from the additive hard-prism system, we plot $(1-\eta)\beta P/\rho$, which must be equal to 1 for additive systems [see Eq. (3.10b)], as a function of density in Fig. 3(d). We can see that the two-state dumbbell fluid produces values lower than 1 at intermediate densities since two dumbbells can get closer to each other in perpendicular orientation than two prisms can, i.e., $\sigma_{13} < (\sigma_1 + \sigma_3)/2$, which manifests in a lower pressure and a higher packing fraction at a given density. Figure 3(d) shows that the PL theory underestimates the effect of non-additivity, producing higher values for $(1-\eta)\beta P/\rho$ than the exact results obtained from the TM and ND methods. Apart from this deviation, the PL theory describes accurately all quantities of the weakly non-additive system of two-state dumbbells.

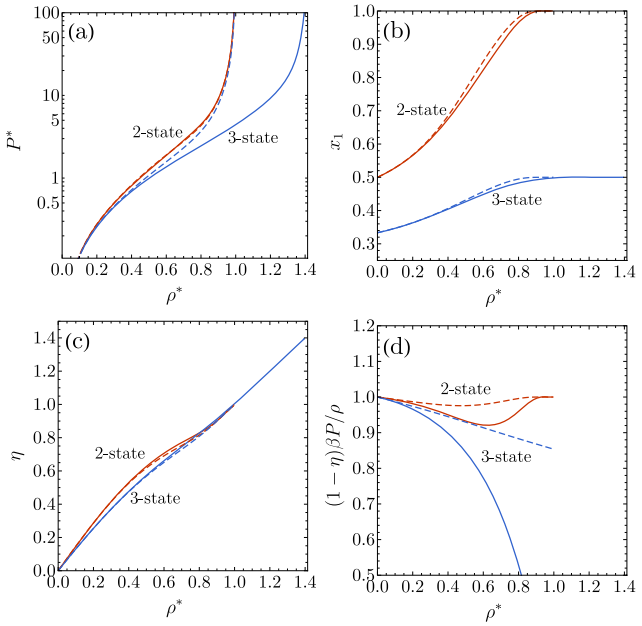

FIG. 3. Phase behavior of hard dumbbells in a q1D channel: (a) pressure, (b) mole fraction, (c) packing fraction, and (d) $(1-\eta)\beta P/\rho$ as functions of the reduced density. Particles can orient along the x and z axes in the two-state model, while the x, y, and z axes are allowed in the three-state one. The dashed curves correspond to the results of the PL theory, while the solid curves are the exact results. The lengths of the dumbbells are chosen as follows: $\sigma_1 = \sigma$, $\sigma_2 = \sigma$, and $\sigma_3 = 2\sigma$. The pressure and density are dimensionless: $P^* = \beta P \sigma_1$ and $\rho^* = \rho\sigma_1$. The corresponding close-packing densities are given by $\rho^*_{cp} = 1$ and $\rho^*_{cp} = \sqrt{2}$ for the two-state and three-state models, respectively. Note that the PL curves do not exist above $\rho^* = 1$.

The phase behavior of the three-state hard dumbbell system is more complicated due to the inclusion of state 2, which is a competitor of state 1 in the ordering process. This can be seen in Fig. 3, where the range of dimensionless density (ρ^*) extends to $\sqrt{2}$ due to the extra orientation state. Therefore, the equation of state of the three-state system deviates substantially from that of the two-state one, as can be seen in Fig. 3(a). We observe that the three-state pressure curve is below the two-state one because there is more space between particles with the inclusion of state 2. This is due to the orientational entropy, which is maximal if the number of particles is the same in all orientations. This entropy term prevails at very low densities, where the system has an isotropic distribution, i.e., $x_1 = x_2 \simeq x_3 \simeq 1/3$. However, the competition between different entropy terms produces orientational ordering in such a way that $x_1 = x_2 \to 1/2$ and $x_3 \to 0$ at close packing, as clearly observed in Fig. 3(b). The orientationally ordered structure develops at $\rho^* \approx 1$, where the average distance between the neighboring particles reduces to σ, which do not allow the particles to occupy a distance 2σ along the z axis, i.e., $x_3 \approx 0$.

One might think naively that the phase behavior of three-state dumbbells becomes identical with that of hard rods of length σ for $\rho^* > 1$ because particles in states 1 and 2 occupy the same distance along the z axis. This idea would be supported by Fig. 3(c), where the curve η vs ρ^* becomes linear for $\rho^* > 1$, as in the fluid of hard rods. However, this equivalence turns out not to be true, since the entropic contributions of $\sigma_{11} = \sigma_{22}$ and σ_{12} contact distances are still dominant for $\rho^* > 1$. The difference between the three-state hard dumbbell and additive hard-body fluids can be visualized with the help of $(1-\eta)\beta P/\rho$, which is shown as a function of density in Fig. 3(d). We can see that the three-state hard dumbbells do not obey $(1-\eta)\beta P/\rho = 1$ because the non-additivity decreases pressure and increases η at a given density, as compared to an additive system. Moreover, it changes sign at $\eta = 1$ (which corresponds to $\rho^* \simeq 1$). Therefore, the equation of state of three-state dumbbells cannot be mapped onto that of hard rods of length σ, even at very high densities. Instead of random orientational ordering of states 1 and 2 along the z axis, the particles form clusters, where neighboring particles are perpendicular to each other, i.e., dimers, trimers, tetramers, . . ., m-mers form with increasing density. At close packing, the length of the cluster must go to infinity and the structure is crossed through the whole system to reach the maximal density. As a consequence, what actually happens is that the three-state dumbbell model for $\rho^* > 1$ becomes progressively closer to hard rods of length $\sigma_{12} = \sigma/\sqrt{2}$, so that $\beta P/\rho \to (1-\rho^*/\sqrt{2})^{-1}$ as density approaches its close-packing value $\rho^*_{cp} = \sqrt{2}$.

Regarding the PL theory as applied to the three-state model, it is accurate for the ordering properties [see Fig. 3(b)], but it fails to predict the crossed structure. This can be seen in the equation of state [see Figs. 3(a) and 3(d)], in which case the pressure of the PL theory diverges at $\rho^* = 1$, precisely where the crossed structure starts to develop.

B. Pair distribution function

We can get more insight into the ordering properties of hard prisms and hard dumbbells by studying the positional pair distribution function along the channel, $g_{ij}(z)$.

1. Hard prisms

As the hard prisms obey the shift property of additive 1D hard-body mixtures [see Eq. (3.28)],[66,79,80] only $g_{11}(z)$ is shown in Fig. 4.

We can see that the prisms become more and more ordered locally and the positional order propagates to larger and larger

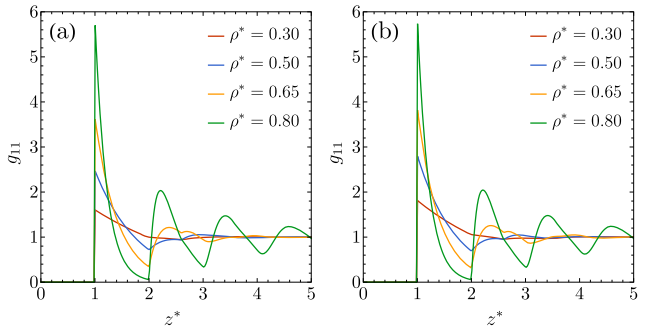

FIG. 4. Pair distribution function between two hard prisms, both having a length σ_1 along the z axis, as a function of distance between the two particles (z^*). The results are shown for (a) two-state and (b) three-state systems for densities $\rho^* = 0.3$, 0.5, 0.65, and 0.8. The other pair distribution functions can be obtained from g_{11} by applying the shift property, Eq. (3.28).

distances with increasing density. At low densities, $g_{11}(z)$ is structureless because the orientational ordering is very weak, while it becomes oscillatory at high density with the period of shortest length (σ_1) due to the development of perfect nematic order with $x_1 = 1$. Therefore, $g_{11}(z)$ becomes identical to $g(z)$ of hard rods having a diameter σ_1 at very high densities. On the other hand, $g_{11}(z)$ is more structured at intermediate densities ($\rho^* = 0.5$ and $\rho^* = 0.65$), where the fractions of particles having lengths σ_2 and σ_3 along the z axis are not negligible. The effects of x_2 and x_3 on $g_{11}(z)$ are present in new singularities at $z = i\sigma_1 + j\sigma_2 + k\sigma_3$, where i, j, k are positive integers [see Eq. (3.29)]. Among those singularities, three of them are kinks at $z = 2\sigma_1$, $\sigma_1 + \sigma_2$, and $\sigma_1 + \sigma_3$ (the latter only in the three-state model), which correspond to $\ell = 2$ in Eqs. (3.25b) and (3.29); the other singularities are of higher order and thus they are not visible in Fig. 4. This shows that $g_{ij}(z)$ cannot be mapped onto an effective hard-rod $g(z)$ with $d = \langle\sigma\rangle$, since in the latter the singularities appear only at multiples of d.

We can also see in Fig. 4 that the pair distribution functions of the two-state and three-state prisms at a common density are almost identical, the main difference being that the three-state prisms are positionally slightly more ordered than the two-state ones at intermediate densities because the three-state system has a higher packing fraction [see Fig. 2(c)].

2. Hard dumbbells

Now we turn our attention to the positional ordering of hard dumbbells. Since the shift property of additive fluids is not valid for hard dumbbells, $g_{11}(z)$, $g_{13}(z)$, and $g_{33}(z)$ are calculated for two-state dumbbells, whereas $g_{11}(z) = g_{22}(z)$, $g_{12}(z)$, $g_{13}(z) = g_{23}(z)$, and $g_{33}(z)$ are considered for the three-state model.

We can see that the shift property of $g_{ij}(z)$ obtained for additive systems is violated even at $\rho^* = 0.3$ in the two-state model, although the shapes of all $g_{ij}(z)$ are very similar [see Fig. 5(a)]. However, the pair distribution functions become very different from each other at high densities [see Fig. 5(b)], since the dumbbells tend to align with their short lengths (σ) along the z axis. The consequence of this fact is that $g_{11}(z)$ becomes very similar to the pair distribution function $g(z)$ of hard rods having a diameter σ, whereas $g_{33}(z)$ shows a second peak higher than the first one at $\rho^* = 0.8$. This peculiar behavior of $g_{33}(z)$ is due to the fact that two dumbbells having lengths 2σ do not like to form a neighboring pair. Opposite to this, $g_{13}(z)$ is very similar to $g_{11}(z)$ because two particles like to form a pair if they have different orientations. In fact, it can be proved from Eq. (3.26) for the two-state model that, in the high-density limit, the shift property $g_{13}(\sigma_{13} + z) \simeq g_{11}(\sigma_1 + z)$ is fulfilled. Also in that limit, $g_{33}(z)$ depletes in the interval $\sigma_3 < z < 2\sigma_{13}$. Beyond $z = 2\sigma_{13}$, $g_{33}(z)$ replicates the behavior of $g_{11}(z)$ for $z > 2\sigma_1$, i.e., $g_{33}(2\sigma_{13} + z) \simeq g_{11}(2\sigma_1 + z)$.

Figures 5(c) and 5(d) show that three-state hard dumbbells behave very differently because the shortest distance between two dumbbells reduces to $\sigma/\sqrt{2}$. At this distance the neighboring particles are perpendicular to each other, and g_{12} has the highest contact value among all g_{ij}. Due to the favorable crossed alignments, the pair distribution functions of the three-state system are more structured than that of the two-state one at both low and high densities. In addition to this, the distance between peaks of g_{ij} is shorter in the three-state model, since the particles can get closer to each other

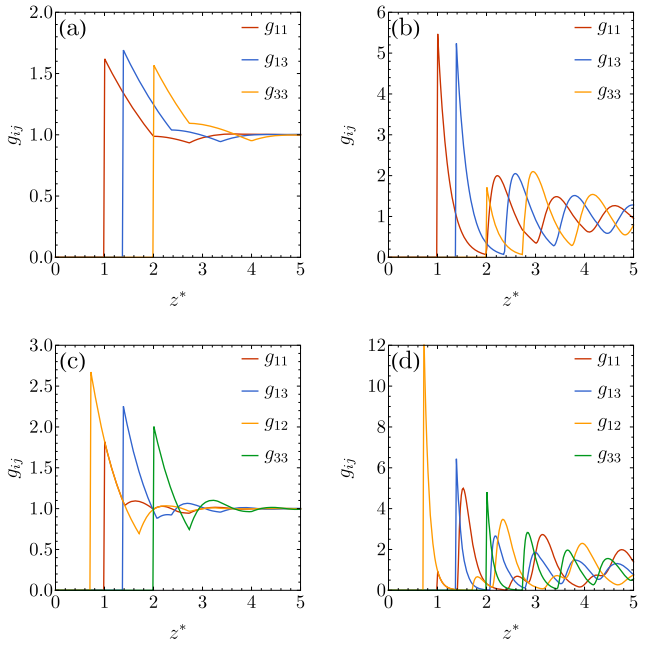

FIG. 5. Pair distribution function between two hard dumbbells, having lengths σ_i and σ_j along the z axis, as a function of distance between the two particles (z^*). The results are shown for (a) the two-state system at $\rho^* = 0.3$, (b) the two-state system at $\rho^* = 0.8$, (c) the three-state system at $\rho^* = 0.6$, and (d) the three-state system at $\rho^* = 1.2$.

in crossed ordering. We can see in Fig. 5(d) that the structures of g_{11} and g_{12} are very special at the high density $\rho^* = 1.2$, because the first, third, fifth, ... peaks of g_{11} (g_{12}) show increasing (decreasing) trends, while the second, fourth, sixth, ... peaks exhibit the opposite trends. Moreover, the second peak of g_{11} (g_{12}) is much higher (smaller) than the first one. Therefore, the trends observed in g_{11} and g_{12} prove that the first neighbors like to be perpendicular, while the second ones tend to be parallel to each other, i.e., particles form crossed clusters in 1-2-1-2-$\cdots$ orientational order. We mention that the distribution functions g_{13} and g_{33} do not provide information about the crossed order, but they show enhanced positional order at $\rho^* = 1.2$.

C. Correlation lengths

The extent of positional order and the propagation of orientational ordering are measured with the help of positional and orientational correlations lengths, which are shown as a function of density in Fig. 6.

1. Hard prisms

The hard prisms are not orientationally correlated because only the highest eigenvalue of the transfer matrix is nonzero, while the other ones are zero. This results in $\xi_o = 0$ for both two- and three-state prisms. The positional correlation of hard prisms (ξ_p) coming from the oscillatory exponential decay of the pair distribution functions [see Eq. (3.30)] has quite a complicate dependence on density because of the crossing of the real part of two poles with different imaginary parts (structural crossover). As a consequence, two kinks

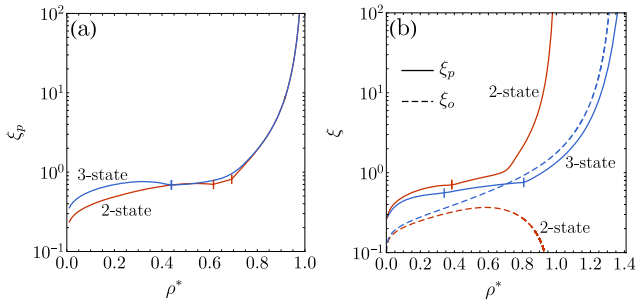

FIG. 6. Orientational (ξ_o) and positional (ξ_p) correlation lengths as functions of density. Results for hard prisms are shown in panel (a), while those for hard dumbbells are shown in panel (b). The vertical bars show the location of kinks apparent in ξ_p.

are present in the two-state prism model, while only one in the three-state one. This can be seen in Fig. 6(a), where the nonmonotonic behavior of ξ_p is shown for both prism models. The presence of kinks and the saturation of ξ_p at intermediate densities may be the result of competition between orientational and positional ordering, because the orientational ordering weakens the positional correlations and shifts the positional ordering towards higher densities. It can also be seen that the three-state system is more correlated than the two-state one at intermediate densities. This may be due to the fact that the three-state system is more packed than the two-state one at a given density, as shown in Fig. 2(c). For densities $\rho^* > 0.8$, both models become equivalent to a 1D hard-rod fluid and, thus, they have the same positional correlation length.

2. Hard dumbbells

Figure 6(b) shows that the positional correlation of hard dumbbells is qualitatively similar to that of hard prisms, with the difference that the two-state dumbbell system has only one kink, while two kinks are present in the three-state model. Moreover, at the same ρ^*, the positional correlation is stronger in the two-state model because it is more packed at a given density [see Fig. 3(c)]. The result of packing effects is that the positional correlation length of hard dumbbells diverges at $\rho^* = 1$ in the two-state model, while this happens at $\rho^* = \sqrt{2}$ in the three-state one. The orientational correlation is very weak and only present at intermediate densities in the two-state system. This is due to the fact that the dumbbells with length 2σ like to form pairs with dumbbells with length σ, but the fraction of the former dumbbells decreases with density. This is not the case in the three-state model, where the orientational correlation length diverges at $\rho^* = \sqrt{2}$.

Therefore, three-state dumbbells exhibit long-range orientational and positional correlation near close packing. This is the consequence of the crossed close-packing structure, where the dumbbells form infinitely long clusters with an orientation sequence 1-2-1-2$\cdots$. We believe that these findings keep being true even in the freely rotating case because the close-packing structure does not change.

V. CONCLUSIONS

In this paper, we have examined the effect of additive and non-additive hard-body interactions on the phase behavior of q1D hard-body fluids, where the particles are allowed to move freely along a straight line and to rotate into a finite number (n) of orientational states. Only two perpendicular orientations are allowed in the two-state model ($n = 2$), while three mutually perpendicular ones are present in the three-state model ($n = 3$). The two-state model can be considered as a minimal model of some single-file fluids placed in a nanopore with rectangular cross section, while the three-state one can represent a single-file fluid in a cylindrical pore.

The additive system has the feature that the contact distance between two particles obeys $\sigma_{ij} = (\sigma_i + \sigma_j)/2$, where σ_i and σ_j are the lengths of a particle with orientations i and j along the z axis, respectively. The prototypes of additive systems are hard spheres, but prisms can also be additive in the above two- and three-state representation. However, some systems can deviate into positive ($\sigma_{ij} \geq (\sigma_i + \sigma_j)/2$) or negative ($\sigma_{ij} \leq (\sigma_i + \sigma_j)/2$) direction from the additive systems. In this regard, the hard-dumbbell model belongs to the class of negative non-additive systems.

We found that the phase behaviors of additive and non-additive systems differ significantly. While the equation of state of additive systems can be mapped onto that of 1D hard rods with an effective length $d = \langle\sigma\rangle$, this is not so for the non-additive systems. We found that $(1-\eta)\beta P/\rho$ can measure the effect of non-additive interaction since that quantity is exactly equal to 1 for all n-state additive systems. By including just one non-additive contact distance, as in the two-state dumbbell model, $(1-\eta)\beta P/\rho$ deviates from 1 only at intermediate densities, since the two-state dumbbell system becomes identical to the fluid of hard rods as it approaches close packing. This comes automatically from the TM method, where $K_{11} = e^{-\beta P\sigma_1}/\beta P$ becomes the dominant matrix element and determines the phase behavior at high pressures, assuming $\sigma_1 = \sigma$ is the shortest contact distance. In the three-state model, the deviation from the 1D hard-rod behavior is much more pronounced due to the presence of $\sigma_{12} = \sigma/\sqrt{2}$. The consequence of this non-additive interaction is that the particles like to form crossed clusters and $(1-\eta)\beta P/\rho$ becomes negative for $\rho^* > 1$. In the three-state dumbbell model, the dominant transfer matrix element is $K_{12} = e^{-\beta P\sigma_{12}}/\beta P$, while the other elements can be neglected at high pressures. It can be easily shown in this limit that the largest and second largest (in absolute) value eigenvalues are $\lambda \to K_{12}$ and $\lambda^* \to -K_{12}$, respectively. Therefore, the resulting equation of state of the system at high pressures is given by $\beta P = \rho/(1 - \rho\sigma/\sqrt{2})$, which corresponds to an equation of state of 1D hard rods having a length $\sigma/\sqrt{2}$. However, the structure is crossed at high pressures and the orientational correlation length diverges since $\xi_o^{-1} = \ln\left(\lambda/|\lambda^*|\right) \to 0$. This argument is strictly valid only in the limit $\beta P \to \infty$, which corresponds to the close-packing density, while the size of the crossed cluster is finite for densities below the close-packing one.

We showed that the general additive q1D fluids can be studied exactly using the PL theory, as well as the TM and ND methods. While the PL theory provides only the bulk properties, such as the equation of state and the orientation order parameter, the TM and ND methods can also be used to determine the local structure of the systems. The study of the structural and bulk properties of q1D hard dumbbells revealed the importance of non-additive interactions,

which can be the driving force in the formation of complex necklace-like structures of anisotropic building blocks, such as the crossed structure. Those systems can be studied exactly using the TM and ND methods, but the PL theory cannot account for the high-density and close-packing structures. Therefore, the success of the PL theory of anisotropic 2D and 3D hard-body fluids may be due to the correct description of side-by-side and end-to-end configurations even if the effect of "T" and other intermediate configurations are incorrectly included into the theory. Regarding the role of the DFT, the exact density functional of additive 1D hard-body n-component mixtures, which was devised by Vanderlick *et al.*,[65] can be applied to one-component anisotropic hard-body fluids with n orientational states using the equal chemical potential condition.[77] It can be shown that hard prisms can be described exactly within the DFT, while hard dumbbells cannot. It is worth noting that the ND method pointed out the weaknesses of the DFT in describing the positive and negative non-additive 1D hard-body mixtures.[81] Therefore, the only possible way to get exact results for more realistic systems, such as the freely rotating q1D rods and single-file fluids in cylindrical pore, is to use the TM and the ND methods. We believe that these exact methods can explain some of the simulation results on the ordering properties of real rod-like nanoparticles, which can move freely in q1D diblock copolymer templates.[82]

Finally, it must be stressed that the results presented in Sec. III are not restricted to the specific two- and three-state prism and dumbbell models, chosen here as prototypes of additive and non-additive systems, respectively. In the case of additive interactions, the high-density phase is equivalent to that of a monocomponent fluid with the smallest length. Interestingly, the same situation occurs if the non-additivity is positive [i.e., $\sigma_{ij} \geq (\sigma_i + \sigma_j)/2$] or if it is negative but the smallest length is smaller than any cross distance σ_{ij}, as happens with the two-state dumbbell model studied in this paper. However, if the smallest cross distance is smaller than the smallest length, then the high-density phase presents the crossed structural ordering exemplified here by the three-state dumbbell model. In this respect, the two-state hard dumbbell model is a caricature version of a model where the dumbbells can freely rotate on the xz plane in a rectangular channel; analogously, if orientation three is removed from our three-state hard dumbbell model, one has a simplification of a more general model in which the dumbbells can freely rotate on the xy plane in a circular channel. Preliminary results show that the orientational and positional correlation lengths of the continuous models are qualitatively similar to those of the discrete models investigated in this paper. Work is currently in progress to study these cases with continuous orientations and the results will be published elsewhere.

ACKNOWLEDGMENTS

A.M.M. and A.S. acknowledge financial support from Grant No. PID2020-112936GB-I00 funded by MCIN/AEI/10.13039/501100011033 and from Grant No. IB20079 funded by Junta de Extremadura (Spain) and by "ERDF A way of making Europe." A.M.M. is also grateful to MCIN/AEI/10.13039/501100011033 and "ESF Investing in your future" for a predoctoral fellowship PRE2021-097702. S.V. and P.G. gratefully acknowledge the financial support of the National Research, Development, and Innovation Office - Grant No. NKFIH K137720 and TKP2021-NKTA-21.

AUTHOR DECLARATIONS

Conflict of Interest

The authors have no conflicts to disclose.

Author Contributions

Ana M. Montero: Formal analysis (supporting); Investigation (equal); Methodology (supporting); Software (lead); Visualization (lead). **Andrés Santos**: Conceptualization (equal); Formal analysis (equal); Funding acquisition (equal); Investigation (equal); Methodology (supporting); Supervision (equal); Writing – original draft (supporting); Writing – review & editing (lead). **Péter Gurin**: Conceptualization (equal); Formal analysis (equal); Funding acquisition (equal); Investigation (equal); Methodology (lead); Validation (equal); Writing – original draft (supporting); Writing – review & editing (supporting). **Szabolcs Varga**: Conceptualization (lead); Formal analysis (equal); Funding acquisition (equal); Investigation (equal); Methodology (equal); Validation (equal); Writing – original draft (lead); Writing – review & editing (supporting).

DATA AVAILABILITY

The data that support the findings of this study are available from the corresponding author upon reasonable request.

REFERENCES

[1] J.-L. Barrat and J.-P. Hansen, *Basic Concepts for Simple and Complex Liquids* (Cambridge University Press, Cambridge, 2003).
[2] L. Mederos, E. Velasco, and Y. Martínez-Ratón, "Hard-body models of bulk liquid crystals," J. Phys.: Condens. Matter **26**, 463101 (2014).
[3] H. H. Wensink, H. Löwen, M. Marechal, A. Härtel, R. Wittkowski, U. Zimmermann, A. Kaiser, and A. M. Menzel, "Differently shaped hard body colloids in confinement: From passive to active particles," Eur. Phys. J.-Spec. Top. **222**, 3023–3037 (2013).
[4] A. B. G. M. Leferink op Reinink, E. van den Pol, A. V. Petukhov, G. J. Vroege, and H. N. W. Lekkerkerker, "Phase behaviour of lyotropic liquid crystals in external fields and confinement," Eur. Phys. J.-Spec. Top. **222**, 3053–3069 (2013).
[5] Q. Zhang, S. Gupta, T. Emrick, and T. P. Russell, "Surface-functionalized CdSe nanorods for assembly in diblock copolymer templates," J. Am. Chem. Soc. **128**, 3898–3899 (2006).
[6] S. Liu, J. B.-H. Tok, J. Locklin, and Z. Bao, "Assembly and alignment of metallic nanorods on surfaces with patterned wettability," Small **2**, 1448–1453 (2006).
[7] W. Li, P. Zhang, M. Dai, J. He, T. Babu, Y.-L. Xu, R. Deng, R. Liang, M.-H. Lu, Z. Nie, and J. Zhu, "Ordering of gold nanorods in confined spaces by directed assembly," Macromolecules **46**, 2241–2248 (2013).
[8] S.-Y. Zhang, M. D. Regulacio, and M.-Y. Han, "Self-assembly of colloidal one-dimensional nanocrystals," Chem. Soc. Rev. **43**, 2301–2323 (2014).
[9] P. Ben Ishai, M. K. Kidder, A. I. Kolesnikov, and L. M. Anovitz, "One-dimensional glassy behavior of ultraconfined water strings," J. Phys. Chem. Lett. **11**, 7798–7804 (2020).
[10] H. Xu, Y. Xu, X. Pang, Y. He, J. Jung, H. Xia, and Z. Lin, "A general route to nanocrystal kebabs periodically assembled on stretched flexible polymer shish," Sci. Adv. **1**, e150002 (2015).

[11] A. N. Generalova, V. A. Oleinikov, and E. V. Khaydukov, "One-dimensional necklace-like assemblies of inorganic nanoparticles: Recent advances in design, preparation and applications," Adv. Colloid Interface Sci. **297**, 102543 (2021).
[12] L. Zhang, G. M. Biesold, C. Zhao, H. Xu, and Z. Lin, "Necklace-like nanostructures: From fabrication, properties to applications," Adv. Mater. **34**, 2200776 (2022).
[13] L. van Hove, "Sur l'intégrale de configuration pour les systèmes de particules à une dimension," Physica **16**, 137–143 (1950).
[14] J. A. Cuesta and A. Sánchez, "General non-existence theorem for phase transitions in one-dimensional systems with short range interactions, and physical examples of such transitions," J. Stat. Phys. **115**, 869–893 (2004).
[15] R. K. Bowles, "A thermodynamic description of the glass transition: An exact one-dimensional example," Physica A **275**, 217–228 (2000).
[16] A. N. Semenov, "Thermodynamic nature of vitrification in a 1D model of a structural glass former," J. Chem. Phys. **143**, 044510 (2015).
[17] Y. Kantor and M. Kardar, "Universality in the jamming limit for elongated hard particles in one dimension," Europhys. Lett. **87**, 60002 (2009).
[18] S. S. Ashwin and R. K. Bowles, "Complete jamming landscape of confined hard discs," Phys. Rev. Lett. **102**, 235701 (2009).
[19] P. C. Hohenberg, "Existence of long-range order in one and two dimensions," Phys. Rev. **158**, 383–386 (1967).
[20] M. Schwartz, "On necklaces with hard non-spherical beads," Physica A **389**, 731–735 (2010).
[21] L. Tonks, "The complete equation of state of one, two and three-dimensional gases of hard elastic spheres," Phys. Rev. **50**, 955–963 (1936).
[22] Z. W. Salsburg, R. W. Zwanzig, and J. G. Kirkwood, "Molecular distribution functions in a one-dimensional fluid," J. Chem. Phys. **21**, 1098–1107 (1953).
[23] A. Drory, "Exact solution of a one-dimensional continuum percolation model," Phys. Rev. E **55**, 3878–3885 (1997).
[24] L. A. Pugnaloni, R. D. Gianotti, and F. Vericat, "Comment on 'Exact solution of a one-dimensional continuum percolation model,'" Phys. Rev. E **56**, 6206–6207 (1997).
[25] P. V. Giaquinta, "Entropy and ordering of hard rods in one dimension," Entropy **10**, 248–260 (2008).
[26] Q. H. Wei, C. Bechinger, and P. Leiderer, "Single-file diffusion of colloids in one-dimensional channels," Science **287**, 625–627 (2000).
[27] A. Pertsinidis and X. S. Ling, "Video microscopy and micromechanics studies of one- and two-dimensional colloidal crystals," New J. Phys. **7**, 33 (2005).
[28] B. H. Lin, M. Meron, B. X. Cui, S. A. Rice, and H. Diamant, "From random walk to single-file diffusion," Phys. Rev. Lett. **94**, 216001 (2005).
[29] O. Bunk, B. Schmitt, B. D. Patterson, P. R. Willmott, C. Padeste, E. Perret, K. Nygård, C. David, A. Diaza, F. Pfeiffera, D. K. Satapathy, and F. J. van der Veen, "Concentration profiles of colloidal fluids in one-dimensional confinement," Chimia **62**, 789 (2008).
[30] B. Lin, D. Valley, M. Meron, B. Cui, H. M. Ho, and S. A. Rice, "The quasi-one-dimensional colloid fluid revisited," J. Phys. Chem. B **113**, 13742–13751 (2009).
[31] M. Kac, "On the partition function of a one-dimensional gas," Phys. Fluids **2**, 8–12 (1959).
[32] M. Kac, G. E. Uhlenbeck, and P. C. Hemmer, "On the van der Waals theory of the vapor–liquid equilibrium. I. Discussion of a one-dimensional model," J. Math. Phys. **4**, 216–228 (1963).
[33] L. M. Casey and L. K. Runnels, "Model for correlated molecular rotation," J. Chem. Phys. **51**, 5070–5089 (1969).
[34] J. Szulga, W. A. Woyczynski, B. Ycart, and J. A. Mann, "The phase transition in a one-dimensional lattice of axisymmetric bodies," J. Stat. Phys. **46**, 67–85 (1987).
[35] S. Saryal, J. U. Klamser, T. Sadhu, and D. Dhar, "Multiple singularities of the equilibrium free energy in a one-dimensional model of soft rods," Phys. Rev. Lett. **121**, 240601 (2018).
[36] S. Saryal and D. Dhar, "Exact results for interacting hard rigid rotors on a *d*-dimensional lattice," J. Stat. Mech. **2022**, 043204.
[37] J. L. Lebowitz, J. K. Percus, and J. Talbot, "On the orientational properties of some one-dimensional model systems," J. Stat. Phys. **49**, 1221–1234 (1987).
[38] Y. Kantor and M. Kardar, "One-dimensional gas of hard needles," Phys. Rev. E **79**, 041109 (2009).
[39] P. Gurin and S. Varga, "Orientational ordering of hard zigzag needles in one dimension," Phys. Rev. E **82**, 041713 (2010).
[40] P. Gurin and S. Varga, "Towards understanding the ordering behavior of hard needles: Analytical solutions in one dimension," Phys. Rev. E **83**, 061710 (2011).
[41] J. F. Marko, "Exact pair correlations in a one-dimensional fluid of hard cores with orientational and translational degrees of freedom," Phys. Rev. Lett. **62**, 543–546 (1989).
[42] C. Tejero and J. Cuesta, "Direct correlation function of a one-dimensional nematic fluid," Physica A **168**, 942–956 (1990).
[43] D. A. Kofke and A. J. Post, "Hard particles in narrow pores. Transfer-matrix solution and the periodic narrow box," J. Chem. Phys. **98**, 4853–4861 (1993).
[44] I. E. Kamenetskiy, K. K. Mon, and J. K. Percus, "Equation of state for hard-sphere fluid in restricted geometry," J. Chem. Phys. **121**, 7355–7361 (2004).
[45] C. Forster, D. Mukamel, and H. A. Posch, "Hard disks in narrow channels," Phys. Rev. E **69**, 066124 (2004).
[46] S. Varga, G. Balló, and P. Gurin, "Structural properties of hard disks in a narrow tube," J. Stat. Mech. **2011**, P11006.
[47] P. Gurin and S. Varga, "Pair correlation functions of two- and three-dimensional hard-core fluids confined into narrow pores: Exact results from transfer-matrix method," J. Chem. Phys. **139**, 244708 (2013).
[48] Y. Hu, L. Fu, and P. Charbonneau, "Correlation lengths in quasi-one-dimensional systems via transfer matrices," Mol. Phys. **116**, 3345–3354 (2018).
[49] A. Huerta, T. Bryk, V. M. Pergamenshchik, and A. Trokhymchuk, "Collective dynamics in quasi-one-dimensional hard disk system," Front. Phys. **9**, 636052 (2021).
[50] A. M. Montero and A. Santos, "Equation of state of hard-disk fluids under single-file confinement," J. Chem. Phys. **158**, 154501 (2023).
[51] A. M. Montero and A. Santos, "Structural properties of hard-disk fluids under single-file confinement," J. Chem. Phys. **159**, 034503 (2023).
[52] M. J. Godfrey and M. A. Moore, "Static and dynamical properties of a hard-disk fluid confined to a narrow channel," Phys. Rev. E **89**, 032111 (2014).
[53] M. J. Godfrey and M. A. Moore, "Understanding the ideal glass transition: Lessons from an equilibrium study of hard disks in a channel," Phys. Rev. E **91**, 022120 (2015).
[54] J. F. Robinson, M. J. Godfrey, and M. A. Moore, "Glasslike behavior of a hard-disk fluid confined to a narrow channel," Phys. Rev. E **93**, 032101 (2016).
[55] Y. Zhang, M. J. Godfrey, and M. A. Moore, "Marginally jammed states of hard disks in a one-dimensional channel," Phys. Rev. E **102**, 042614 (2020).
[56] Y. Hu and P. Charbonneau, "Comment on 'Kosterlitz-Thouless-type caging-uncaging transition in a quasi-one-dimensional hard disk system,'" Phys. Rev. Res. **3**, 038001 (2021).
[57] P. Gurin, S. Varga, and G. Odriozola, "Anomalous structural transition of confined hard squares," Phys. Rev. E **94**, 050603 (2016).
[58] L. Fu, C. Bian, C. W. Shields, D. F. Cruz, G. P. López, and P. Charbonneau, "Assembly of hard spheres in a cylinder: A computational and experimental study," Soft Matter **13**, 3296–3306 (2017).
[59] W. Jin, H. K. Chan, and Z. Zhong, "Shape-anisotropy-induced ordered packings in cylindrical confinement," Phys. Rev. Lett. **124**, 248002 (2020).
[60] W. Jin, Y. Wang, H.-K. Chan, and Z. Zhong, "Confinement-induced columnar crystals of ellipses," Phys. Rev. Res. **3**, 013053 (2021).
[61] E. Basurto, P. Gurin, S. Varga, and G. Odriozola, "Anisotropy-independent packing of confined hard ellipses," J. Mol. Liq. **333**, 115896 (2021).
[62] R. Fantoni and A. Santos, "One-dimensional fluids with second nearest-neighbor interactions," J. Stat. Phys. **169**, 1171–1201 (2017).
[63] D. Liarte, A. Petri, and S. Salinas, "Hard-needle elastomer in one spatial dimension," Braz. J. Phys. **53**, 73 (2023).
[64] J. K. Percus, "Equilibrium state of a classical fluid of hard rods in an external field," J. Stat. Phys. **15**, 505–511 (1976).
[65] T. K. Vanderlick, H. T. Davis, and J. K. Percus, "The statistical mechanics of inhomogeneous hard rod mixtures," J. Chem. Phys. **91**, 7136–7145 (1989).
[66] M. Schmidt, "Fundamental measure density functional theory for nonadditive hard-core mixtures: The one-dimensional case," Phys. Rev. E **76**, 031202 (2007).
[67] J. K. Percus, "Density functional theory of single-file classical fluids," Mol. Phys. **100**, 2417–2422 (2002).

[68]C. Barrio and J. R. Solana, "Binary mixtures of additive hard spheres. Simulations and theories," in *Theory and Simulation of Hard-Sphere Fluids and Related Systems*, *Lecture Notes in Physics*, edited by A. Mulero (Springer-Verlag, Berlin, 2008), Vol. 753, pp. 133–182.
[69]J. D. Parsons, "Nematic ordering in a system of rods," Phys. Rev. A **19**, 1225–1230 (1979).
[70]S. Lee, "A numerical investigation of nematic ordering based on a simple hard-rod model," J. Chem. Phys. **87**, 4972–4974 (1987).
[71]S. C. McGrother, D. C. Williamson, and G. Jackson, "A re-examination of the phase diagram of hard spherocylinders," J. Chem. Phys. **104**, 6755–6771 (1996).
[72]P. J. Camp, C. P. Mason, M. P. Allen, A. A. Khare, and D. A. Kofke, "The isotropic–nematic phase transition in uniaxial hard ellipsoid fluids: Coexistence data and the approach to the Onsager limit," J. Chem. Phys. **105**, 2837–2849 (1996).
[73]S. Varga and I. Szalai, "Parsons-Lee theory and a simulation-based study of two-dimensional hard-body fluids," J. Mol. Liq. **85**, 11–21 (2000).
[74]G. J. Vroege and H. N. W. Lekkerkerker, "Phase transitions in lyotropic colloidal and polymer liquid crystals," Rep. Prog. Phys. **55**, 1241 (1992).
[75]B. Groh and S. Dietrich, "Orientational order in dipolar fluids consisting of nonspherical hard particles," Phys. Rev. E **55**, 2892–2901 (1997).
[76]P. Padilla and E. Velasco, "The isotropic-nematic transition for the hard Gaussian overlap fluid: Testing the decoupling approximation," J. Chem. Phys. **106**, 10299–10310 (1997).
[77]L. Onsager, "The effects of shape on the interaction of colloidal particles," Ann. N. Y. Acad. Sci. **51**, 627–659 (1949).
[78]A. Santos, *A Concise Course on the Theory of Classical Liquids: Basics and Selected Topics*, *Lecture Notes in Physics* (Springer, New York, 2016), Vol. 923.
[79]C. Grodon, M. Dijkstra, R. Evans, and R. Roth, "Decay of correlation functions in hard-sphere mixtures: Structural crossover," J. Chem. Phys. **121**, 7869–7882 (2004).
[80]C. Grodon, M. Dijkstra, R. Evans, and R. Roth, "Homogeneous and inhomogeneous hard-sphere mixtures: Manifestations of structural crossover," Mol. Phys. **103**, 3009–3023 (2005).
[81]A. Santos, "Exact bulk correlation functions in one-dimensional nonadditive hard-core mixtures," Phys. Rev. E **76**, 062201 (2007).
[82]Q.-y. Tang and Y.-q. Ma, "Self-assembly of rod-shaped particles in diblock-copolymer templates," J. Phys. Chem. B **113**, 10117–10120 (2009).